

# Pavement Distress Evaluation Along Steep-To-Rolling Highway Sections:

## *A Case Study of Mau Summit-Timboroa*

\*Moses Wytey Gasaya, Simpson Nyambane Osano and John Francis Gichaga

Received on 26<sup>th</sup> June, 2025; Received in revised form 24<sup>th</sup> July, 2025; Accepted on 4<sup>th</sup> August, 2025.

### Abstract

*This study evaluates pavement distresses along the 39-km Mau Summit-Timboroa section of Kenya's A8 highway in steep-to-rolling terrain to enhance infrastructure durability and safety. Objectives include assessing distress types, analysing contributions of traffic loading, speed, material properties, and road gradient to deterioration, and identifying cost-effective pavement designs. Using ASTM D6433 and Kenyan Road Design Manual standards, field surveys, laboratory testing, and layered elastic analysis identified fatigue cracking, rutting, and potholes, yielding a Pavement Condition Index (PCI = 73, Satisfactory). Traffic loading, measured as 37.5 million Equivalent Single Axle Loads (ESALs) over a 5-year projection and 18,581 ESALs per day in 2024, low vehicle speeds (19–23 km/h), weak asphalt concrete (AC, left-hand side (LHS):  $[\tau]_1 = 0.595\text{--}0.946$  MPa; right-hand side (RHS):  $[\tau]_1 = 0.911\text{--}1.561$  MPa), dense bituminous macadam (DBM, LHS:  $[\tau]_2 = 0.363\text{--}0.665$  MPa; RHS:  $[\tau]_2 = 0.511\text{--}0.893$  MPa), and steep gradients (4.5–9.7%) drove severe LHS rutting (27.66–38.04 mm) and moderate RHS rutting (2.17–9.94 mm) after 5 years. High shear stresses (LHS AC: 0.439–0.480 MPa) and temperatures (40°C) exacerbate distress. The stable graded crushed stone (GCS) subbase ( $[\tau]_3 = 0.284\text{--}0.55$  MPa) contributes minimally. A cost-benefit analysis recommends rigid pavements for high-traffic, steep sections (e.g., Timboroa, 9.7%), polymer-modified asphalt, increased layer thicknesses (AC  $\geq 65$  mm, DBM  $\geq 200$  mm), and drainage improvements. Applicable to global highways like Ethiopia's Rift Valley, these findings optimize maintenance, safety, and durability.*

**Keywords:** Pavement distress, steep-to-rolling terrain, pavement condition index, traffic loading, cost-benefit analysis, road gradient, flexible pavement, maintenance optimization, asphalt pavement.

### INTRODUCTION

Flexible pavements in steep-to-rolling terrains face accelerated deterioration due to heavy traffic loading, steep gradients, and environmental factors, posing challenges for infrastructure longevity and safety. The 39-km Mau Summit-Timboroa section of the A8 highway (previously A104) in Kenya, a critical link connecting Nairobi to western Kenya and Uganda, exemplifies these challenges. Managed by the Kenya National Highways Authority (KeNHA), this segment experiences high traffic volumes, with 18,581 Equivalent Single Axle Loads (ESALs) per day in 2024 and 37.5 million ESALs over 5 years, and variable slopes (4.5–9.7%, **Figure 1**), contributing to severe pavement distress, including rutting, fatigue cracking, and potholes. Severe left-hand side (LHS) rutting (27.66–38.04 mm, **Figure 2**)

and moderate right-hand side (RHS) rutting (2.17–9.94 mm, **Figure 3**) after 5 years are driven by weak asphalt concrete (AC, LHS:  $[\tau]_1 = 0.595\text{--}0.946$  MPa; RHS:  $[\tau]_1 = 0.911\text{--}1.561$  MPa) and dense bituminous macadam (DBM, LHS:  $[\tau]_2 = 0.363\text{--}0.665$  MPa; RHS:  $[\tau]_2 = 0.511\text{--}0.893$  MPa) layers under heavy traffic and high temperatures (40°C). The mean Pavement Condition Index (PCI = 73, Satisfactory, **Table 1**) masks localized deterioration on steep slopes (e.g., Timboroa, 9.7%, **Figure 4**), necessitating targeted interventions.

This study evaluates pavement distresses along the Mau Summit-Timboroa section, using ASTM D6433 (**Table 1**) for PCI assessment and the Kenyan Road Design Manual (Ministry of Transport and Communications, 1988) for

\*Corresponding author:

Moses Wytey Gasaya Student, MSc Civil Engineering (Transportation Engineering), Department of Civil and Construction Engineering, University of Nairobi.  
Email: waytey@students.uonbi.ac.ke

structural design. Field surveys, laboratory testing, and layered elastic analysis (LEA) quantify distress mechanisms, particularly LHS rutting (e.g., 38.04 mm at Timboroa, **Figure 5**) driven by AC (58.7–59.7%) and DBM (37.0–37.4%) under low truck speeds (19–23 km/h) and deceleration ( $2 \text{ m/s}^2$ ). The stable graded crushed stone (GCS) subbase ( $[\tau]_3 = 0.284\text{--}0.55 \text{ MPa}$ ) contributes minimally (3.2–14.1%). A cost-benefit analysis compares flexible and rigid pavements, recommending polymer-modified asphalt, increased layer

thicknesses ( $\text{AC} \geq 65 \text{ mm}$ ,  $\text{DBM} \geq 200 \text{ mm}$ ), and drainage improvements. Findings apply to global highways in regions like Ethiopia's Rift Valley or the Andes, informing KeNHA's infrastructure planning (Kenya Gazette, 2016).

## THEORY

Pavement deterioration in steep terrains is driven by heavy traffic, steep gradients, and environmental factors, accelerating distress

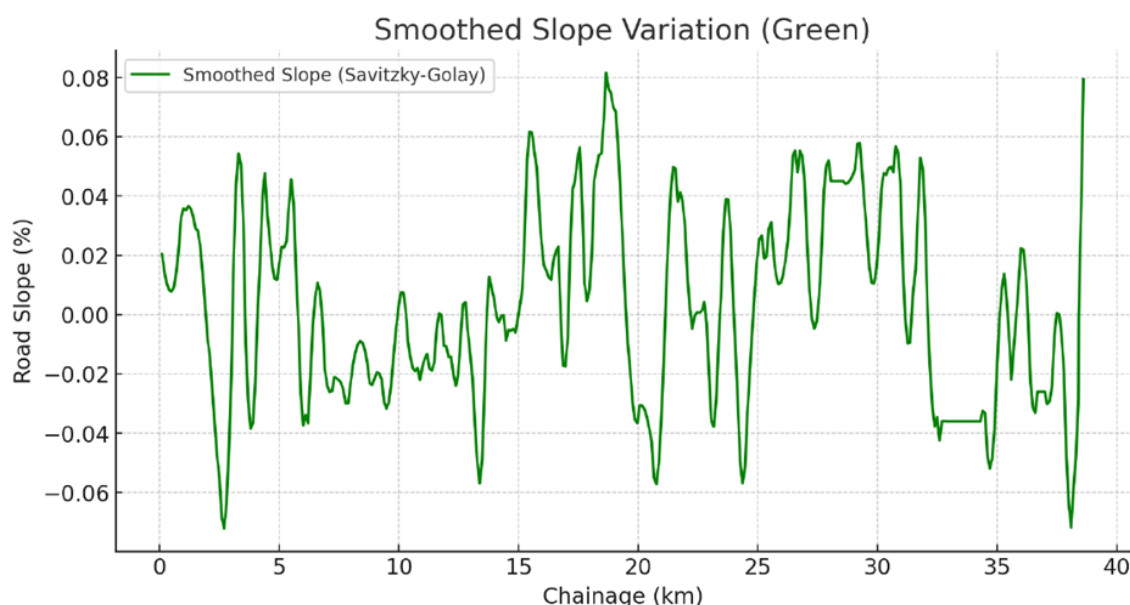


**FIGURE 1**

Smoothed slope variation graph

Source: Field survey, 2025

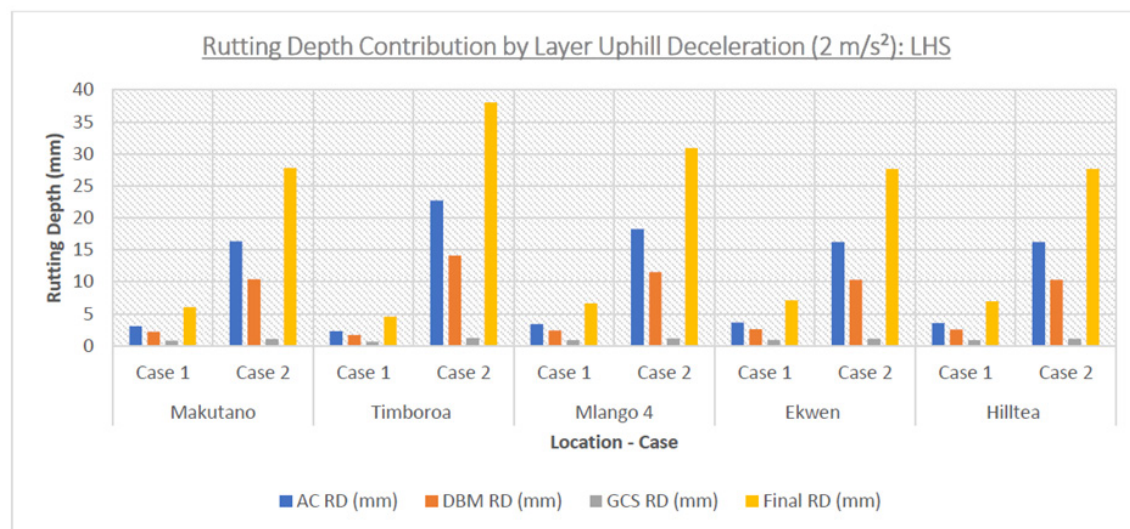


**FIGURE 2**

Rutting depth contributions by layer (LHS, uphill deceleration,  $2 \text{ M/S}^2$ )

Source: LEA Analysis, 2025

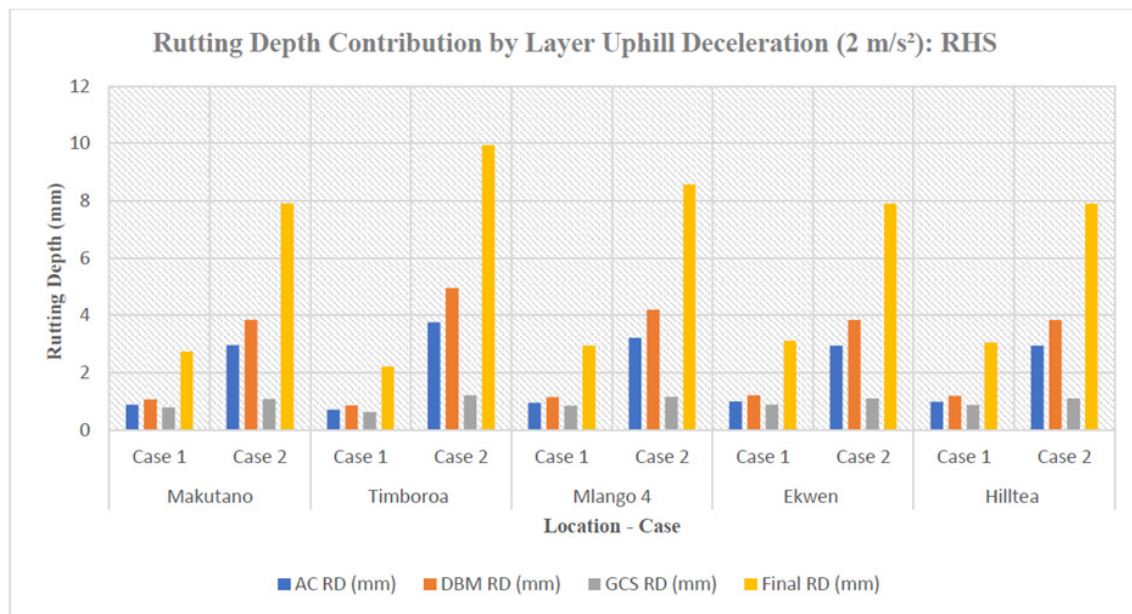


**FIGURE 3**  
Rutting depth contributions by layer (RHS, uphill deceleration, 2 M/S<sup>2</sup>)  
**Source:** LEA Analysis, 2025

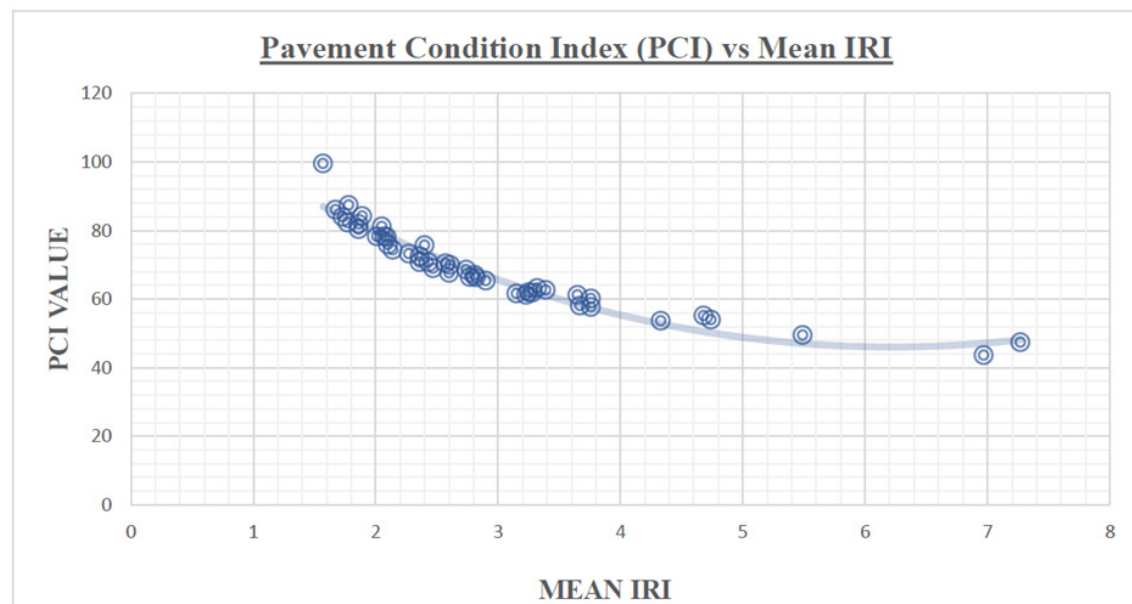


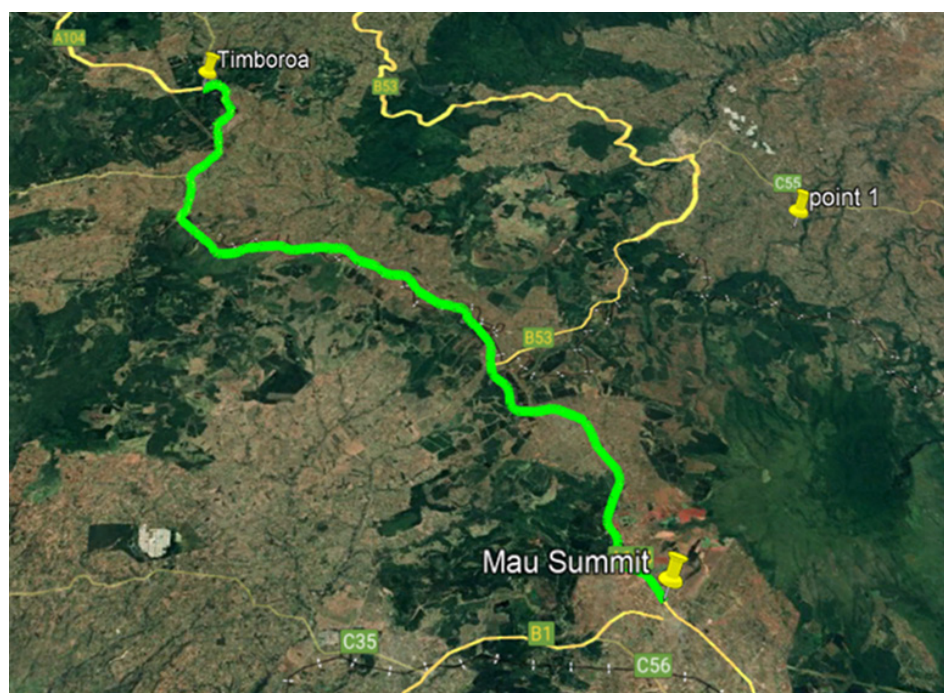
**FIGURE 4**  
PCI vs. IRI for ascending slopes >5.0%  
**Source:** ASTM D6433 Analysis, 2025

like rutting and fatigue cracking. This review synthesizes studies and standards, focusing on design, materials, traffic, and maintenance, aligned with ASTM D6433 (2020) and the Kenyan Road Design Manual (Ministry of Transport and Communications, 1988).

Pavement design standards emphasize robust

structures for steep terrains. AASHTO (2014, 2016) provides geometric and soil classification guidelines, while Huang (2004) advocates mechanistic-empirical designs for gradients (4.5–9.7%) and heavy axle loads. Traffic loading significantly impacts deterioration, with Liddle's (1962) Equivalent Axle Load Factor (EALF) quantifying axle load effects, critical for the A8's



**FIGURE 5**

Map of Mau Summit-Timboroa highway section

**Source:** Google earth pro. 2025**TABLE 1**

Pavement Condition Index (PCI) Scale, ASTM D6433-98

PCI Range scale	Rating colour	Pavement Condition
85-100	Green	Good
70-85	Light Green	Satisfactory
55-70	Yellow	Fair
40-55	Orange	Poor
25-40	Red	Very Poor
10-25	Dark Red	Serious
0-10	Grey	Failed

**Source:** ASTM D6433-98, 1998

37.5 million ESALs. Overloading (15,000 kg) increases shear stress by ~55%, causing severe rutting (27.66–38.04 mm) at low speeds (19–23 km/h) (Al-Qadi & Wang, 2011; Wang & Al-Qadi, 2013; Kim & Lee, 2016).

Material properties mitigate distress. High temperatures (40–45°C) reduce AC cohesion (0.4–0.7 MPa), exacerbating rutting, while polymer-modified asphalt enhances shear strength ( $[\tau]_1 \geq 0.911$  MPa) and reduces air voids (AC <4%) (Brown & Brunton, 1986; Sousa et al., 1991;

Monismith, 1992; Ceylan et al., 2008; Zhang & Li, 2002). Poor drainage ( $\mu < 0.5\%$ ) worsens distress, with improved drainage ( $\mu > 0.6\%$ ) protecting subbase layers (Paterson, 1987; Thom, 2014; Ahmed & Erlingsson, 2015).

Advanced evaluation techniques, such as ground-penetrating radar (Loulizi & Al-Qadi, 2004) and machine learning (Gao & Li, 2019; Li et al., 2011), improve distress analysis. Maintenance strategies favor rigid pavements (25–30-year lifespan) for high-traffic, steep sections and increased layer

thicknesses (AC  $\geq$  65 mm, DBM  $\geq$  200 mm) for durability (Hajek & Haas, 1997; Ullidtz, 1998).

## RESEARCH METHODS

### Study Area

The 39-km Mau Summit-Timboroa section of the A8 highway spans Baringo and Nakuru Counties, Kenya, forming part of the Northern Corridor linking Mombasa to Kigali. This segment features steep-to-rolling terrain with slopes ranging from 4.5% to 9.7%. Key locations—Makutano (5.8%), Timboroa Bridge (9.7%), Mlango 4 (5.7%), Ekwen (4.5%), and Hill Tea (4.8%)—were selected for their variable gradients and distress patterns. The section experiences high traffic volumes (18,581 ESALs/day in 2024, 37.5 million ESALs over 5 years), contributing to significant pavement deterioration (**Figure 5**).

### Data Collection

#### Field Surveys

Visual inspections per ASTM D6433-20 identified distress types (rutting, fatigue cracking, potholes) (**Figures 6a, 6b, 6c, 6d, 6e**), supplemented by automated image processing (Li et al., 2011). Geological surveys used AASHTO M 145-91 and ASTM D3282-15 for soil classification and CBR tests (subgrade CBR 10–25, S3–S5).

### Traffic and Axle Load Surveys

Traffic was measured over seven days using pneumatic tube counters. Axle load surveys followed Overseas Road Note 40 (Transport Research Laboratory, 2004), calculating EALF per Liddle

$$(1962): EALF = \left( \frac{L_s}{8200} \right)^{4.5} \text{ (Equation 1).}$$

where  $L_s$  is the axle load kilograms (Liddle, 1962). Heavy goods vehicles (HGVs, VEF = 8.76) dominated, with overloading up to 15,000 kg noted.



6a) Longitudinal cracking observed on the road



6b) Ravelling long the road



6c) Pothole cluster in the transition zone between steep and rolling terrain



6d) Rut formation along the climbing sections





6e) Rutting along the climbing lane section

**FIGURE 6 a-e**

Pavement distresses on Mau Summit-Timboroa Highway

Source: Field survey, 2025

**Pavement Performance**

IRI was measured using a high-speed inertial profiler (mean: 2.3 m/km, range: 1.0–7.9 m/km) (Sayers & Karamihas, 1998). Rutting depths (RD) were assessed per ASTM E1703-17, with LHS RDs of 27.66–38.04 mm and RHS RDs of 2.17–9.94 mm. Slope-specific RDs are detailed in **Table 13**.

**Structural Surveys**

Deflection measurements used a Falling Weight Deflectometer (FWD) per ASTM D4694-09. Ground-penetrating radar (GPR) assessed layer thickness (Loulizi & Al-Qadi, 2004). Trenching and coring sampled materials, following Kenyan Road Design Manual protocols (Ministry of Transport and Communications, 1988). The LHS pavement comprises 54 mm AC ( $E = 6385$  MPa,  $[\tau]_1 = 0.595$ – $0.946$  MPa), 155 mm DBM ( $E = 5222$  MPa,  $[\tau]_2 = 0.363$ – $0.665$  MPa), and 270 mm GCS ( $E = 3867$  MPa,  $[\tau]_3 = 0.284$ – $0.55$  MPa). The RHS comprises 50 mm AC ( $E = 6385$  MPa,  $[\tau]_1 = 0.911$ – $1.561$  MPa), 180 mm DBM ( $E = 5222$  MPa,  $[\tau]_2 = 0.511$ – $0.893$  MPa), and 270 mm GCS ( $E = 3867$  MPa,  $[\tau]_3 = 0.284$ – $0.55$  MPa).

**Road Gradient and Speed Surveys**

GPS devices and total stations measured elevation changes to calculate slopes (4.5–9.7%). Traffic speed surveys focused on HGVs, using radar guns to determine average speeds (19–23 km/h) on steep ascents (**Tables E1, Appendix E**).

**Data Analysis**

Pavement distress data were analysed using statistical and mechanistic methods to evaluate traffic loading, road gradient, and material properties. Statistical methods included regression analysis to model relationships between distress types and variables like traffic volume, gradient, and layer properties. Pearson correlation analysis examined associations between gradient, speed, and distress, using:

$$r = \frac{\sum(x-\bar{x})(y-\bar{y})}{\sqrt{\sum(x-\bar{x})^2 \sum(y-\bar{y})^2}} \quad (\text{Equation 2}).$$

where (x) and (y) represent paired variables (e.g., gradient and proportion of speeders), and  $\bar{x}$  and  $\bar{y}$  are their means. Road gradient data were smoothed using the Savitzky-Golay filter (Python, `scipy.signal.savgol_filter`, 11-point window, second-order polynomial; Savitzky & Golay, 1964). (**Appendix G**)

Mechanistic analysis employed LEA to model shear stress under a 10,000 kg axle load (98,100 N,  $q = 0.8$  MPa, tire radius  $a = 0.14$  m). The rutting depth (RD) model integrated slope ( $L_p = 0.505$ ), truck speed (19–23 km/h), shear stress ( $\tau$ )<sub>1</sub>, shear strength ( $[\tau]_1$ ), temperature (40°C), and axle loads (37.5M ESALs). Two scenarios were modelled: Case 1 (horizontal shear in AC only) and Case 2 (scaled horizontal shear across all layers). The RD equation is:

$$RD = (1 + L_p) \cdot \sum_{i=1}^n 10^{-7.6422} \cdot T_i^{3.7586} \cdot \left( \frac{N}{1+5.5572V^{1.2219}} \right)^{0.8358} \cdot (\tau_i/[\tau]_i)^{0.6526} \quad (\text{Equation 3}),$$

where RD is rutting depth (mm),  $T_i = 40^\circ\text{C}$ ,  $N = 37.5\text{M}$ ,  $V = 19\text{--}23\text{ km/h}$ ,  $\tau_i$  and  $[\tau]_i$  are layer-specific (**Table 11**). Results were evaluated against ASTM D6433 (<6 mm: low, 6–15 mm: moderate, >15 mm: high) and Kenyan standards (<10 mm). A cost-benefit analysis compared flexible and rigid pavements, assessing construction costs, maintenance, and lifespan (Hajek & Haas, 1997).

## RESULTS

### Visual and Surface Condition

Visual and surface condition surveys of the 39-km Mau Summit-Timboroa A8 highway were conducted using the Hawkeye 2000 system with four pavement and asset-logging cameras,

following ASTM D6433-20 (**Table 1**) and the Kenyan Road Design Manual (Ministry of Transport and Communications, 1988). Major distresses included isolated potholes, rutting, longitudinal cracking, and patches, with minor distresses like asphalt bleeding and aggregate loss not indicating structural failure (**Table A1, Appendix A**). The International Roughness Index (IRI) averaged 2.3 m/km (range: 1.0–7.9 m/km) (**Table 2**) for both lanes, with rut depths averaging 3.2 mm in 2024 (left-hand side [LHS]: 27.66–38.04 mm, **Figure 5**; right-hand side RHS: 2.17–9.94 mm after 5 years, projected from 2024; **Figure 6**). The Pavement Condition Index (PCI), calculated per ASTM D6433-20 (**Table 1**), averaged 73 (Satisfactory, range: 35.2–98.7) (**Table 3**).

**TABLE 2**

Mean roughness measurements (IRI)

Roughness Measurements (IRI)					
Mau Summit-Timboroa A8	Points	Min. IRI M/Km	Max of IRI M/Km	Mean IRI, M/Km	Mean IRI
LHS	380	1.0	7.9	2.3	2.3
RHS	378	1.0	7.7	2.3	

Source: ASTM E1703-17, 2024 2025

**TABLE 3**

Rut depth and PCI summary

Rut Depth and PCI Summary				
Road section	Average IRI	Average Rut	PCI Value	Rating
Mau Summit-Timboroa A8	2.3	3.2	73	Satisfactory

Source: ASTM E1703-17, 2024 2025

### Traffic and Axle Load Surveys

Traffic surveys recorded an average daily traffic (ADT) of 4,053 equivalent standard axles (ESAs) in 2024, with heavy goods vehicles (HGVs, VEF = 8.76) predominant and overloading up to 15,000 kg (**Table 4**). At the Timboroa–Naibkoi Junction, 2024 daily ESAs were 16,396 (RHS) and 18,581 (LHS) (**Table 4, Table B1, Appendix B**). The cumulative ESA (CESA) for 2024 was 37.5 million ESAs for the LHS and 33.1 million ESAs for the RHS, used for rutting analysis, with projections indicating increased loading over time (**Tables 5a, 5b, and 6**).

### Structural Condition

Coring Test Results: Core and logging results for

surfacing and base layers are detailed in (**Tables C1, C2, D1 (Appendices C, D)**).

Subgrade Material Test Results: Subgrade testing at km 13+500 (LHS) and km 33+500 (RHS) showed California Bearing Ratio (CBR) values of 10–25 (S3–S5 classification), with plastic mass (PM) ranging from 630–972 kg/m<sup>3</sup> and plasticity index (PI) from 14–18% (**Table 7**).

Deflection measurements (FWD) (**Table F1**) and GPR: The LHS pavement comprises 54 mm asphalt concrete (AC,  $E = 6385\text{ MPa}$ ,  $[\tau]_1 = 0.595\text{--}0.946\text{ MPa}$ ), 155 mm dense bituminous macadam (DBM,  $E = 5222\text{ MPa}$ ,  $[\tau]_2 = 0.363\text{--}0.665\text{ MPa}$ ), and 270 mm graded crushed stone (GCS,  $E = 3867$

**TABLE 4**

Vehicle equivalence factors and daily ESAs

TYPE	Average Daily Traffic	Vehicle Equivalence Factor (LHS)	Daily Equivalent Standard Axles	Average Daily Traffic	Vehicle Equivalence Factor (RHS)	Daily Equivalent Standard Axles
OB	137.65	1.63	224	67.26	1.63	109
BUS	199.60	1.53	305	177.63	1.53	271
LGV	211.77	0.02	5	140.90	0.02	3
MGV	811.94	2.01	1631	623.66	2.01	1253
HGV-1	1345.79	3.44	4626	271.84	3.44	934
HGV-2	1345.79	8.76	11791	1577.95	8.76	13825
<b>TOTAL</b>	<b>4052.54</b>		<b>18581</b>	<b>2859.24</b>		<b>16396</b>

Source: Axle Load Survey, 2025

**TABLE 5a**

Traffic projections (LHS)

DESIGN PERIOD	ANNUAL TRAFFIC GROWTH RATE (LHS)					
	4.00%	5.00%	6.00%	7.00%	8.00%	9.00%
5	36,733,740.40	37,475,076.80	38,231,015.07	39,001,767.63	39,787,548.53	40,588,573.43
7	53,566,584.31	55,219,463.31	56,927,380.12	58,691,955.79	60,514,849.08	62,397,757.01
10	81,425,952.28	85,303,826.37	89,392,737.30	93,703,764.33	98,248,510.69	103,039,124.8
15	135,800,861.57	146,346,777.60	157,858,662.57	170,426,144.47	184,146,843.79	199,127,039.13
20	201,956,252.79	224,254,770.78	249,481,514.97	278,033,251.51	310,359,676.37	346,970,205.91

Source: Axle Load Survey, 2025

**TABLE 5b**

Traffic projections (RHS)

DESIGN PERIOD	ANNUAL TRAFFIC GROWTH RATE (RHS)					
	4.00%	5.00%	6.00%	7.00%	8.00%	9.00%
5	32,413,590.03	33,067,739.97	33,734,774.50	34,414,881.05	35,108,248.50	35,815,067.14
7	47,266,771.21	48,725,259.82	50,232,313.41	52,683,532.03	53,397,870.38	55,059,334.88
10	71,849,678.41	75,271,486.80	78,879,512.58	150,382,812.00	86,693,783.74	90,920,987.39
15	119,829,709.81	129,135,350.75	139,293,355.78	245,334,554.29	162,489,859.03	175,708,276.35
20	178,204,754.26	197,880,807.19	220,140,705.99	245,334,554.29	273,859,160.57	306,164,030.21

Source: Axle Load Survey, 2025



**TABLE 6**

Projected traffic with traffic class

Traffic Station/Road Section	Base year	Base Year DESA	Design Period (Years)	Projected Traffic Loading			Traffic Class
				Growth Rate/ CESA (Millions)			
				4.00%	5.00%	6.00%	
Mau Summit-Timboroa	2024	18,581	5(2029)	36.7	37.5	38.2	T1
			10(2034)	81.4	85.3	89.3	T0
			15 (2039)	135.8	146.3	157.9	T0
			20 (2044)	202.0	224.3	278.8	TX

Source: Axle Load Survey, 2025

**TABLE 7**

Subgrade test results

S/No.	Clients Ref.	Reference							Atterberg Limits					Compaction T 99			
									LL	PL	PI	LS	PM	MDD	OMC	4 days	Swell
			20 mm	10 mm	5 mm	2mm	425 µm	75 µm	(%)	(%)	(%)	(%)		( Kg/m³ )	(%)	soak	
			(ROAD 1) Mau Summit- Timboroa Road														
1	Km 13+500 LHS	Top Subgrade	100	95	86	68	54	35	53	35	18	9	972	1385	22.2	12	0.1
2	Km 13+500 LHS	Bottom Subgrade	100	93	84	60	48	30	50	32	18	9	864	1390	24.0	18	0.1
3	Km 33+500 RHS	Top Subgrade	100	88	77	63	46	28	40	23	17	9	782	1622	14.6	25	0.1
4	Km 33+500 RHS	Bottom Subgrade	100	90	79	63	45	33	43	29	14	7	630	1492	21.2	10	0.1

Source: Ministry of Transport, Infrastructure, Housing, Urban Development & Public Works Materials Testing & Research Department.

MPa,  $[\tau]_3 = 0.284\text{--}0.55$  MPa). The RHS comprises 50 mm AC ( $E = 6385$  MPa,  $[\tau]_1 = 0.911\text{--}1.561$  MPa), 180 mm DBM ( $E = 5222$  MPa,  $[\tau]_2 = 0.511\text{--}0.893$  MPa), and 270 mm GCS ( $E = 3867$  MPa,  $[\tau]_3 = 0.284\text{--}0.55$  MPa). Mean elastic moduli are 6385 MPa (AC), 5222 MPa (DBM), 3867 MPa (GCS), and 292 MPa (subgrade) (Table 8). Section-specific overlay requirements are in Table 9.

#### Road Gradient and slope

Elevation ranges from 2457 m to 2842 m, with

slopes from -8.1% to 9.7% (average uphill: 3.5%; downhill: -2.7%). Slopes are categorized as flat (<2%: 10%), rolling (2–5%: 72%), and steep (>5%: 18%) (Table F2, Figure F1 and F2, Appendix F). Steep sections (e.g., Timboroa: 9.7%, Makutano: 5.8%) and sharp transitions (e.g., Boito–Timboroa) increase shear stress, correlating with severe LHS rutting (e.g., 38.04 mm at Timboroa) (Table F1, Appendix F).

**TABLE 8**

Pavement layer moduli across four sections

Road ID	HS	Elastic Modulus (Mpa)			
		Surfacing	Base	Subbase	Subgrade
<b>A8 (1)</b>	Km 0.0-3.0	5533	4664	6147	333
	Km 3.0-10.0	7320	5663	3112	307
	Km 10.0-14.0	6302	5338	2344	236
	Km 14.0-39.0	6709	6085	6134	254
	<b>Mean</b>	<b>6385</b>	<b>5222</b>	<b>3867</b>	<b>292</b>

Source: FWD Surveys, 2025

**TABLE 9**

Overlay requirements (mm)

Road ID	HS	Overlay Requirements (mm)	
		7-year Overlay	15-year Overlay
MAUSUMMIT - TIMBOROA	Km 0.0-3.0	33	62
	Km 3.0-10.0	16	35
	Km 10.0-14.0	21	39
	Km 14.0-39.0	12	29
	Mean	20	41

Source: FWD Surveys, 2025.

**Gradient and Pavement Distress Analysis**

Pavement condition was assessed using ASTM D6433-98 (**Table 1**), with a mean Pavement Condition Index (PCI) of 73 (Satisfactory), International Roughness Index (IRI) of 2.3 m/km (range: 1.0–7.9 m/km). Rutting depth (RD) averaged 3.2 mm in 2024, with left-hand side (LHS) rutting ranging from 27.66–38.04 mm (**Figure 5**) and right-hand side (RHS) rutting from 2.17–9.94 mm (**Figure 6**) after 5 years. Slope-specific RD ranges include 4.51–27.66 mm (moderate ascending, 3.0–5.0%), 5.25–38.04 mm (steep ascending, >5.0%), 2.17–6.00 mm (moderate descending, -3.0% to -5.0%), and 2.22–6.42 mm (steep descending, <-5.0%, **Figure 3**). Severe LHS rutting occurs at Timboroa (38.04 mm), Ekwen (27.66 mm), and Mlango 4 (27.79 mm), driven by weak AC ( $[\tau]_1 = 0.595\text{--}0.946$  MPa, 58.7–59.7%) and DBM ( $[\tau]_2 = 0.363\text{--}0.665$  MPa, 37.0–37.4%). RHS rutting is moderate due to higher shear strengths (AC:  $[\tau]_1 = 0.911\text{--}1.561$  MPa; DBM:  $[\tau]_2 = 0.511\text{--}0.893$  MPa) and thicker DBM (180 mm) (**Table 10-13**, **Table F1-7**, **Appendix F**).

**Ascending Slopes**

Moderate Slopes (3.0%–5.0%): PCI ranges from 43.41–92.02, IRI from 1.41–7.15 m/km, with RDs generally low (<6 mm, ASTM-compliant) except in high-traffic zones (e.g., Ekwen: LHS RD 27.66 mm, **Figure 5**). Routine maintenance (e.g., sealing) suffices, but areas with IRI >4.5 m/km need targeted repairs. (**Tables 10-11**, **Table F1-7**, **Appendix F**).

Steep Slopes (>5.0%): PCI ranges from 43.69–49.53, IRI from 6.97–7.27 m/km (**Figure 4**), with severe LHS RDs (e.g., Timboroa: 38.04 mm, Mlango 4: 27.79 mm, **Figure 5**) exceeding ASTM (>15 mm) and Kenyan (<10 mm) thresholds.

High shear stresses (LHS AC: 0.439–0.480 MPa; DBM: 0.274–0.300 MPa) and low safety margins (AC: 0.115–0.507 MPa; DBM: 0.063–0.391 MPa) require rehabilitation with polymer-modified asphalt and increased layer thicknesses. (**Tables 10-13**, **Table F1-7**, **Appendix F**).

**Descending Slopes**

Moderate Slopes (-3.0% to -5.0%): PCI ranges from 42.42–98.72, IRI from 1.27–7.48 m/km, with RDs typically low (<6 mm). Localized repairs are needed where IRI >4.5 m/km (e.g., Timboroa: RHS RD 9.94 mm, **Figure 6**). (**Tables 10-13**, **Table F1-7**, **Appendix F**).

Steep Slopes (< -5.0%): PCI ranges from 35.72–76.84, IRI up to 8.3 m/km, with isolated severe RDs (e.g., 6.415 mm at -7.5%) requiring rehabilitation. LHS distress is less severe than on ascending slopes due to lower shear stresses during descent (**Figure 3**). (**Table 10-11**, **Table F1**, **F2**, **F3**, **Appendix F**).

**Observations and Trends**

Steeper slopes correlate with higher IRI ( $r = 0.59$ ) and lower PCI ( $r = -0.74$ ). LHS RDs at Timboroa (38.04 mm), Ekwen (27.66 mm), and Mlango 4 (27.79 mm) exceed ASTM (>15 mm) and Kenyan (<10 mm) thresholds, driven by high temperatures (45°C) reducing AC cohesion (LHS: 0.4–0.7 MPa; RHS: 0.6–1.9 MPa) and overloading (15,000 kg) increasing shear stress by ~55% (e.g., LHS AC: 0.74 MPa). RHS RDs (e.g., Timboroa: 9.94 mm) are moderate due to thicker DBM (180 mm) and higher shear strengths. The GCS subbase ( $[\tau]_3 = 0.284\text{--}0.55$  MPa) contributes minimally to rutting (LHS: 3.2–4.0%; RHS: 12.3–14.1%). (**Table 10-13**, **Table F1-7**, **Appendix F**).

**Influence of Slope and Speed on Shear Stress**

**TABLE 10**

Recommended maintenance actions by slope category

Slope Category	Intervention	Materials	Specifications	Cost-Benefit Notes
<b>Moderate</b> (3.0–5.0%, -3.0 to -5.0%)	Routine Main-tenance	Sealing, Patching	Maintain PCI >70, IRI <4.5 m/km	Cost-effective; ex-tends lifespan by 5–7 years
<b>Steep</b> (>5.0%, <-5.0%)	LHS Rehabili-tation	Polymer-Modified Asphalt, Rigid Pavements	AC: E ≥7000 MPa, cohesion ≥1.0 MPa, ≥65 mm; DBM: ≥200 mm; Air voids: AC <4%, DBM <6%	Rigid pavements (20–30-year lifes-pan) preferred for high-traffic zones (e.g., Timboroa)
<b>Steep</b> (>5.0%, <-5.0%)	RHS Targeted Maintenance	Polymer-Modified Asphalt	AC: E ≥7000 MPa, cohesion ≥1.0 MPa; Drainage: $\mu >0.6$	Reduces RDs (7.90–9.94 mm) cost-effec-tively
<b>General</b>	Axle Load Limits, Drain-age, GCS Stabilization	Cement-Treated GCS	Axle load ≤10,000 kg; Drainage: $\mu >0.6$ ; GCS: $[\tau]_3=0.27-0.53$ MPa (wet)	Mitigates AC/DBM rutting, enhances durability

**Notes:** Interventions address severe LHS RDs (27.66–38.04 mm) and moderate RHS RDs (7.90–9.94 mm) per Table 6. Rigid pavements reduce maintenance costs in steep sections [18].

**Source:** Cost-Benefit Analysis, 2025

**TABLE 11**

Pavement layer properties and shear strength

Side	Layer	Thickness (mm)	Elastic Modulus (MPa)	Shear Strength $[\tau]_1$ (MPa)	Air Voids (%)
<b>LHS</b>	AC	54	6385	0.595–0.946	6.8
	DBM	155	5222	0.363–0.665	7.0
	GCS	270	3867	0.284–0.550	N/A
<b>RHS</b>	AC	50	6385	0.911–1.561	3.0
	DBM	180	5222	0.511–0.893	6.3
	<b>GCS</b>	<b>270</b>	<b>3867</b>	<b>0.284–0.550</b>	<b>N/A</b>

**Notes:** AC = Asphalt Concrete, DBM = Dense Bituminous Macadam, GCS = Graded Crushed Stone. Subgrade (CBR 10–25, S3–S5) excluded from rutting analysis. Shear strength ranges reflect variability across test locations. Air voids data explain LHS distress severity.

**Source:** FWD and GPR Surveys, 2025

### and Rutting

Road gradients (4.5–9.7%, **Figure 3**) and low truck speeds (19–23 km/h) were analysed for a three-layered pavement. LHS consists of 54 mm AC (E = 6385 MPa,  $[\tau]_1 = 0.595-0.946$  MPa), 155 mm DBM (E = 5222 MPa,  $[\tau]_2 = 0.363-0.665$  MPa), and 270 mm GCS (E = 3867 MPa,  $[\tau]_3 = 0.284-0.55$  MPa) (**Table 11**). RHS has 37 mm AC (E = 6385 MPa,  $[\tau]_1 = 0.911-1.561$  MPa), 180 mm DBM (E = 5222 MPa,  $[\tau]_2 = 0.511-0.893$  MPa), and 270 mm GCS (**Table 11**). Shear stress peaks in LHS AC (0.439–

0.480 MPa) and DBM (0.274–0.300 MPa) (**Table 12, Table F3**) under deceleration ( $3 \text{ m/s}^2$ ) at steep slopes (e.g., Timboroa: 9.7%, **Figure 3**), with low safety margins (AC: 0.115–0.507 MPa; DBM: 0.063–0.391 MPa). RHS shows robust margins (AC: 0.431–1.122 MPa; DBM: 0.231–0.619 MPa). High temperatures ( $45^\circ\text{C}$ ) and overloading (15,000 kg) amplify LHS distress (**Figure 5, Table 10-13, Table F1-7, Appendix F**).

### Rutting Predictions after 5 years

*Case 1 (Acceleration):* LHS RDs: 4.51–6.96 mm



TABLE 12

Shear stress by layer and location uphill deceleration (2 m/s<sup>2</sup>)

Location	Slope (%)	Side	Layer	Shear Stress $\tau_i$ (MPa)	Safety Margin $[\tau]_i - \tau_i$ (MPa)
Timboroa Bridge	9.7	LHS	AC	0.480	0.115–0.466
			DBM	0.300	0.063–0.365
			GCS	0.080	0.204–0.470
		RHS	AC	0.480	0.431–1.081
			DBM	0.300	0.211–0.593
			GCS	0.080	0.204–0.470
Makutano	5.8	LHS	AC	0.439	0.156–0.507
			DBM	0.274	0.089–0.391
		RHS	AC	0.439	0.472–1.122
			DBM	0.274	0.237–0.619
Mlango 4	5.7	LHS	AC	0.448	0.147–0.498
			DBM	0.280	0.083–0.385
		RHS	AC	0.448	0.463–1.113
			DBM	0.280	0.231–0.613
Ekwen	4.5	LHS	AC	0.439	0.156–0.507
			DBM	0.274	0.089–0.391
		RHS	AC	0.439	0.472–1.122
			DBM	0.274	0.237–0.619
Hill Tea	4.8	LHS	AC	0.439	0.156–0.507
			DBM	0.274	0.089–0.391
		RHS	AC	0.439	0.472–1.122
			DBM	0.274	0.237–0.619

**Notes:** Shear stress calculated using LEA (10,000 kg axle,  $q=0.8$  MPa). Overloading (15,000 kg) increases stress by ~50% (e.g., LHS AC: 0.720 MPa). High temperatures (40°C) reduce LHS AC cohesion to 0.4–0.7 MPa. GCS margins consistent across locations.

**Source:** LEA Analysis, 2025

(AC: 38.6–49.2%; DBM: 37.3–37.5%) (**Figure 5, Table 13, Table F4, Appendix F**); RHS RDs: 2.17–3.7 mm (DBM: 38.7–39.2%; AC: 37.6–37.4%) (**Figure 6, Table F4, Appendix F**).

**Case 2 (Deceleration):** LHS RDs: 37.66–88.04 mm (AC: 38–38.7%; DBM: 37.0–30.4%) (**Figure 5, Table 13, Table F6-F7, Appendix F**); RHS RDs:

2.90–7.94 mm (DBM: 37.6–39.9%; AC: 37.3–37.9%) (**Figure 6, Table F6-F7, Appendix F**). LHS Case 2 RDs exceed ASTM (>15 mm) and Kenyan (<10 mm) thresholds.

#### Location-Specific Observations

Timboroa (9.7%) has the highest LHS RD (38.04 mm, Case 2), driven by AC (59.7%) and DBM

**TABLE 13**

Location-specific rutting depths and layer contributions

Location/ Slope (%)	Side	Total RD (mm)	AC Contribution	DBM Contribution	GCS Contribution	Severity (ASTM D6433)
<b>Timboroa Bridge (9.7%)</b>	LHS	38.04	59.7% (22.72 mm)	37.4% (14.09 mm)	3.2% (1.22 mm)	High (>15 mm)
	RHS	9.94	37.9% (3.77 mm)	49.9% (4.96 mm)	12.3% (1.22 mm)	Moderate (6–15 mm)
<b>Makutano (5.8%)</b>	LHS	27.79	58.7% (16.31 mm)	37.4% (10.39 mm)	3.9% (1.09 mm)	High (>15 mm)
	RHS	7.91	37.3% (2.95 mm)	48.6% (3.84 mm)	14.1% (1.12 mm)	Moderate (6–15 mm)
<b>Mlango 4 (5.7%)</b>	LHS	27.79	58.7% (16.31 mm)	37.4% (10.39 mm)	3.9% (1.09 mm)	High (>15 mm)
	RHS	8.57	37.3% (3.20 mm)	49.0% (4.20 mm)	13.7% (1.17 mm)	Moderate (6–15 mm)
<b>Ekwen (4.5%)</b>	LHS	27.66	58.7% (16.23 mm)	37.0% (10.32 mm)	4.0% (1.11 mm)	High (>15 mm)
	RHS	7.90	37.3% (2.95 mm)	48.6% (3.84 mm)	14.1% (1.11 mm)	Moderate (6–15 mm)
<b>Hill Tea (4.8%)</b>	LHS	27.66	58.7% (16.23 mm)	37.0% (10.32 mm)	4.0% (1.11 mm)	High (>15 mm)
	RHS	7.90	37.3% (2.95 mm)	48.6% (3.84 mm)	14.1% (1.11 mm)	Moderate (6–15 mm)

**Notes:** ASTM D6433 thresholds: <6 mm (low), 6–15 mm (moderate), >15 mm (high). Kenyan standard: <10 mm. LHS RDs exceed both standards, indicating urgent rehabilitation needs.

**Source:** ASTM D6433-20, 2025

(37.4%) (**Figure 5**). Ekwen (4.5%, 27.66 mm) and Mlango 4 (5.7%, 27.79 mm) show severe LHS RDs due to high shear stresses and low safety margins. RHS RDs are moderate (e.g., Timboroa: 9.94 mm, **Figure 6**), reflecting better compaction (AC air voids: 3.0% vs. LHS 6.8%) and thicker DBM. Makutano (5.8%) and Hill Tea (4.8%) follow similar LHS trends, with GCS contributing minimally. (**Table 13**, **Table F3**, **Appendix F**).

#### Implications for Pavement Design

Steep slopes (>5.0%) and low speeds (19–23 km/h) exacerbate LHS rutting due to weak AC/DBM and high air voids (AC: 6.8%). RHS benefits from thicker DBM and higher shear strengths, reducing RDs by 25–40%. Recommendations include polymer-modified asphalt ( $E \geq 7$  MPa, cohesion  $\geq 2$  MPa), increased thicknesses (AC  $\geq 65$  mm, DBM  $\geq 200$  mm), drainage improvements ( $\mu > 0.55\%$ ), and rigid pavements for high-traffic sections. Findings apply globally to steep

terrains (e.g., Ethiopia's Rift Valley) (Monismith, 1992). This pavement distress evaluation enables agencies to prioritize interventions, optimizing resource allocation and resilience.

#### DISCUSSION

This study evaluates pavement distress along the 39-km Mau Summit-Timboroa section of Kenya's A8 highway, focusing on rutting after 5 years. Severe LHS rutting (27.66–38.04 mm; **Figure 5**) and moderate RHS rutting (2.17–9.94 mm; **Figure 6**) driven by steep gradients (4.5–9.7%, **Figure 3**), heavy traffic (37.5 million ESALs), weak materials, and high temperatures (40–45°C). These findings align with ASTM D6433 (**Table 1**) and the Kenyan Road Design Manual (Ministry of Transport and Communications, 1988). Severe LHS rutting, particularly at Timboroa (38.04 mm, 9.7% slope), Ekwen (27.66 mm, 4.5%), and Mlango 4 (27.79 mm, 5.7%) (**Figure 5**), results from weak asphalt

concrete (AC:  $[\tau]_1 = 0.595\text{--}0.946$  MPa, 58.7–59.7%) and dense bituminous macadam (DBM:  $[\tau]_2 = 0.363\text{--}0.665$  MPa, 37.0–37.4%) under high shear stresses (AC: 0.439–0.480 MPa; DBM: 0.274–0.300 MPa). RHS rutting is moderate (e.g., Timboroa: 9.94 mm, **Figure 6**) due to higher shear strengths (AC:  $[\tau]_1 = 0.911\text{--}1.561$  MPa; DBM:  $[\tau]_2 = 0.511\text{--}0.893$  MPa) and thicker DBM (180 mm). Steep slopes (>5.0%) correlate with lower PCI (35.7–49.5) and higher IRI (6.97–8.3 m/km) (**Figure 4**), consistent with Huang (2004).

### Primary Findings and Literature Comparison

Severe LHS rutting, particularly at Timboroa (38.04 mm, 9.7% slope), Ekwen (27.66 mm, 4.5%), and Mlango 4 (27.79 mm, 5.7%), results from weak asphalt concrete (AC:  $[\tau]_1 = 0.595\text{--}0.946$  MPa, 58.7–59.7%) and dense bituminous macadam (DBM:  $[\tau]_2 = 0.363\text{--}0.665$  MPa, 37.0–37.4%) under high shear stresses (AC: 0.439–0.480 MPa; DBM: 0.274–0.300 MPa). This aligns with Al-Qadi and Wang (2011) and Wang and Al-Qadi (2013), who report that overloading (15,000 kg) increases shear stress by ~55%, exacerbating rutting at low speeds (19–23 km/h). RHS rutting is moderate (e.g., Timboroa: 9.94 mm) due to higher shear strengths (AC:  $[\tau]_1 = 0.911\text{--}1.561$  MPa; DBM:  $[\tau]_2 = 0.511\text{--}0.893$  MPa) and thicker DBM (180 mm), consistent with Brown and Brunton (1986) and Monismith (1992), who emphasize the role of material properties in mitigating distress. The stable graded crushed stone (GCS) subbase ( $[\tau]_3 = 0.284\text{--}0.55$  MPa) contributes minimally (LHS: 3.2–4.0%; RHS: 12.3–14.1%), supporting Paterson's (1987) findings on subbase stability. High temperatures (45°C) reduce AC cohesion (0.4–0.7 MPa), amplifying LHS rutting, as noted by Sousa et al. (1991) and Zhang and Li (2002). Poor drainage ( $\mu < 0.5\%$ ) exacerbates distress, aligning with Ahmed and Erlingsson (2015), while improved drainage ( $\mu > 0.6\%$ ) could mitigate subgrade softening.

Steep slopes (>5.0%) correlate with lower PCI (35.7–49.5) and higher IRI (6.97–8.3 m/km), consistent with Huang (2004) and Kim and Lee (2016), who highlight gradient impacts on pavement performance. The Case 2 model (deceleration) accurately predicts severe LHS RDs exceeding ASTM (>15 mm) and Kenyan (<10 mm) thresholds, supporting mechanistic-empirical approaches (Huang, 2004). RHS's moderate RDs align with Kenyan standards in most cases,

reflecting better compaction (AC air voids: 3.0% vs. LHS 6.8%), as per Brown and Brunton (1986).

### Deviations from Literature

The study's finding of severe LHS rutting (e.g., 38.04 mm at Timboroa) exceeds typical values in flatter terrains (6–15 mm) reported by Sousa et al. (1991), likely due to the A8's steep gradients (9.7%) and sharp transitions (e.g., Boito–Timboroa). The minimal GCS contribution (3.2–14.1%) deviates from Thom (2014), who suggests higher subbase influence in wet conditions, possibly due to the A8's relatively stable subgrade (CBR 10–25).

### Cost-Benefit Implications

Rigid pavements are cost-effective for steep, high-traffic sections (e.g., Timboroa), aligning with Hajek and Haas (1997). Polymer-modified asphalt and increased layer thicknesses (AC  $\geq 65$  mm, DBM  $\geq 200$  mm) are viable for LHS rehabilitation, supported by Monismith (1992) and Zhang and Li (2002). Drainage improvements ( $\mu > 0.6\%$ ) and axle load limits ( $\leq 10,000$  kg) reduce maintenance costs, as per Paterson (1987) and Kenya Gazette (2016).

### CONCLUSION

This study confirms that steep-to-rolling terrains along the 39-km Mau Summit–Timboroa segment of A8 highway significantly exacerbate deterioration, driven by weak LHS AC ( $[\tau]_1 = 0.595\text{--}0.946$  MPa, 54 mm) and DBM ( $[\tau]_2 = 0.363\text{--}0.665$  MPa, 155 mm) under heavy traffic loads (37.5 million ESALs) and steep gradients (4.5–9.7%, **Figure 3**). The LHS exhibits severe rutting depths (37.66–88.04 mm, **Figure 5**), particularly at Timboroa (9.7%, 38.04 mm), Ekwen (4.5%, 27.66 mm), and Mlango 4 (5.7%, 27.79 mm), with AC (58.7–59.7%) and DBM contributing significantly (37.0–37.4%). The RHS pavement (50 mm AC,  $[\tau]_1 = 0.911\text{--}1.561$  MPa; 180 mm DBM,  $[\tau]_2 = 0.511\text{--}0.893$  MPa) shows moderate rutting (2.7–9.9 mm, **Figure 6**), with DBM (48.6–49.9%) and AC (37.3–37.9%) remaining ASTM D6433-compliant (**Table 1**) in most cases. Steeper grades (e.g., 9.7% at Timboroa, **Figure 3**) and low truck speeds (19–23 km/h) during deceleration increase shear stress in LHS AC (0.439–0.480 MPa) and DBM (0.274–0.300 MPa), with low safety margins (AC: 0.115–0.507 MPa; DBM: 0.063–0.391 MPa). The cost-benefit analysis favours rigid pavements for high-traffic



sections (e.g., Timboroa), with findings applicable globally to regions like Ethiopia's Rift Valley.

Steeper grades (e.g., 9.7% at Timboroa, 5.8% at Makutano) and low truck speeds (19–23 km/h) during deceleration increase shear stress in LHS AC (0.439–0.480 MPa) and DBM (0.274–0.300 MPa), with low safety margins (AC: 0.115–0.507 MPa; DBM: 0.063–0.391 MPa). High air voids (LHS: AC: 6.8%, DBM: 7.0%) and environmental factors—high temperatures (45°C) reducing LHS AC cohesion to 0.4–0.7 MPa and overloading (15,000 kg) increasing stresses by ~55%—exacerbate deterioration at Timboroa, Ekwen, and Mlango 4. The Case 2 model predicts critical LHS RDs, exceeding ASTM (>15 mm) and Kenyan (<10 mm) thresholds, necessitating urgent rehabilitation. RHS's higher DBM shear strengths and thicker DBM reduce RDs by 25–37%. Moderate slopes (3.0–5.0%) sustain satisfactory conditions (PCI: 56.3–98.7, RDs: 1.27–7.48 mm), requiring maintenance, while steep slopes (>5.0%) exhibit poor performance (PCI: 35.7–49.5, RDs: 6.97–8.3 m/km), demanding robust interventions.

The cost-benefit analysis favours rigid pavements for high-traffic sections (e.g., Timboroa Bridge–Mlango 4–Boito–Timboroa), with 25–30-year lifespans compared to 7–15 years for flexible pavements (Fernando & Liu, 2002).

This study confirms that steep-to-rolling terrains along the 39-km Mau Summit–Timboroa section of Kenya's A8 highway exacerbate pavement deterioration, driven by weak LHS AC ( $[\tau]_1 = 0.595$ – $0.946$  MPa) and DBM ( $[\tau]_2 = 0.363$ – $0.665$  MPa) under heavy traffic (37.5 million ESALs) and steep gradients (4.5–9.7%). Severe LHS rutting (27.66–38.04 mm) at Timboroa (9.7%), Ekwen (4.5%), and Mlango 4 (5.7%) exceeds ASTM and Kenyan thresholds, while RHS rutting (2.17–9.94 mm) remains moderate. Recommendations include rigid pavements for steep sections, polymer-modified asphalt, increased layer thicknesses, and drainage improvements, applicable globally to regions like Ethiopia's Rift Valley.

## RECOMMENDATIONS

To address severe pavement distress along the 39-km Mau Summit–Timboroa section of Kenya's A8 highway:

i) Rigid Pavements for Steep Sections: Implement

rigid pavements (25–30-year lifespan) at slopes >5.0% (e.g., Timboroa, 9.7%) to reduce maintenance costs (Hajek & Haas, 1997).

- ii) LHS Rehabilitation: Use polymer-modified asphalt ( $E \geq 7$  MPa) and increase AC ( $\geq 65$  mm) and DBM ( $\geq 200$  mm) thicknesses at Timboroa, Ekwen, and Mlango 4 (Monismith, 1992).
- iii) RHS Maintenance: Apply routine maintenance (e.g., sealing) for moderate RHS rutting (e.g., Timboroa: 9.94 mm).
- iv) Improve Drainage: Upgrade drainage to achieve  $\mu \geq 0.6\%$  to protect the GCS subbase and prevent subgrade softening, reducing distress risks.
- v) Axle Load Limits: Enforce  $\leq 10,000$  kg axle loads to reduce shear stress (Kenya Gazette, 2016).
- vi) Stabilize GCS Subbase: Cement-stabilize the GCS subbase to maintain shear strength in wet conditions, ensuring structural integrity.

These recommendations address LHS distress, optimize RHS maintenance, and align with cost-effective rigid pavements and polymer-modified asphalt solutions. Applicable globally to regions like Ethiopia's Rift Valley, they ensure resilient infrastructure for KeNHA.

## CITED REFERENCES

- Ahmed, A. W., & Erlingsson, S. (2015).** Numerical validation of viscoelastic responses of a pavement structure in a full-scale accelerated pavement test. *International Journal of Pavement Engineering*, 16(8), 656–667. Retrieved from <https://doi.org/10.1080/10298436.2014.943209>
- Al-Qadi, I. L., & Wang, H. (2011).** Evaluation of pavement damage due to new tire designs. *Computer-Aided Civil and Infrastructure Engineering*, 26(5), 333–346. Retrieved from <https://doi.org/10.1111/j.1467-8667.2010.00694.x>
- American Association of State Highway and Transportation Officials. (2014).** *A policy on geometric design of highways and streets*. Washington, DC: Author.
- American Association of State Highway and Transportation Officials. (2016).** *Standard specification for classification of soils for highway construction (AASHTO M 145-91)*. Washington,

DC: Author.

**ASTM International. (2016).** *Standard practice for classification of soils and soil-aggregate mixtures for highway construction purposes (ASTM D3282-15)*. West Conshohocken, PA: Author. Retrieved from <https://doi.org/10.1520/D3282-15>

**ASTM International. (2017).** *Standard test method for measuring rut-depth of pavement surfaces using a straightedge (ASTM E1703-17)*. West Conshohocken, PA: Author. Retrieved from <https://doi.org/10.1520/E1703-17>

**ASTM International. (2019).** *Standard test method for deflections with a falling-weight-type impulse load (ASTM D4694-09)*. West Conshohocken, PA: Author. Retrieved from <https://doi.org/10.1520/D4694-09>

**ASTM International. (2020).** *Standard practice for roads and parking lots pavement condition index surveys (ASTM D6433-20)*. West Conshohocken, PA: Author. Retrieved from <https://doi.org/10.1520/D6433-20>

**Brown, S. F., & Brunton, J. M. (1986).** An introduction to the analytical design of bituminous pavements. *Highway Engineering*, 33(4), 3–15. Retrieved from <https://doi.org/10.1111/j.1467-6346.1986.tb00789.x>

**Ceylan, H., Gopalakrishnan, K., & Kim, S. (2008).** Advanced approaches to hot-mix asphalt dynamic modulus prediction. *Canadian Journal of Civil Engineering*, 35(7), 699–707. Retrieved from <https://doi.org/10.1139/L08-005>

**Fernando, E. G., & Liu, W. (2002).** Development of a simplified mechanistic pavement design procedure. *Computer-Aided Civil and Infrastructure Engineering*, 17(5), 347–359. Retrieved from <https://doi.org/10.1111/1467-8667.00281>

**Gao, Y., & Li, X. (2019).** Machine learning-based pavement performance prediction. *Computer-Aided Civil and Infrastructure Engineering*, 34(10), 865–879. Retrieved from <https://doi.org/10.1111/mice.12456>

**Hajek, J. J., & Haas, R. C. G. (1997).** Economic evaluation of pavement maintenance strategies.

*Journal of Transportation Engineering*, 123(3), 171–179. Retrieved from [https://doi.org/10.1061/\(ASCE\)0733-947X\(1997\)123:3\(171\)](https://doi.org/10.1061/(ASCE)0733-947X(1997)123:3(171))

**Huang, Y. H. (2004).** *Pavement analysis and design* (2nd ed.). Upper Saddle River, NJ: Pearson Education.

**Kenya Gazette. (2016).** *Legal notice no. 2*. Nairobi, Kenya: Government Printer. Retrieved from <https://www.kenyalaw.org/gazettes/2016>

**Kim, J. S., & Lee, S. W. (2016).** Reliability-based pavement design under heavy traffic. *Structural Control and Health Monitoring*, 23(4), 632–647. Retrieved from <https://doi.org/10.1002/stc.1802>

**Liddle, W. J. (1962).** Application of AASHO road test results to the design of flexible pavements. In *Proceedings of the International Conference on Structural Design of Asphalt Pavements* (pp. 42–51). Ann Arbor, MI: University of Michigan.

**Li, Q., Xiao, D. X., & Wang, K. C. P. (2011).** Automated pavement distress evaluation using image processing. *Computer-Aided Civil and Infrastructure Engineering*, 26(6), 423–435. Retrieved from <https://doi.org/10.1111/j.1467-8667.2010.00703.x>

**Loulizi, A., & Al-Qadi, I. L. (2004).** Application of ground-penetrating radar in pavement evaluation. *Journal of Transportation Engineering*, 130(6), 749–757. Retrieved from [https://doi.org/10.1061/\(ASCE\)0733-947X\(2004\)130:6\(749\)](https://doi.org/10.1061/(ASCE)0733-947X(2004)130:6(749))

**Ministry of Transport and Communications. (1988).** *Kenyan road design manual, part III: Materials and pavement design for new roads*. Nairobi, Kenya: Author. Retrieved from <https://transport.go.ke/node/3367>

**Monismith, C. L. (1992).** Analytically based asphalt pavement design and rehabilitation. *Journal of Transportation Engineering*, 118(5), 611–628. Retrieved from [https://doi.org/10.1061/\(ASCE\)0733-947X\(1992\)118:5\(611\)](https://doi.org/10.1061/(ASCE)0733-947X(1992)118:5(611))

**Paterson, W. D. O. (1987).** *Road deterioration and maintenance effects*. New York, NY: Wiley.

**Sayers, M. W., & Karamihas, S. M. (1998).** *The little book of traffic profiling*. Ann Arbor, MI:

University of Michigan Transportation Research Institute.

**Savitzky, A., & Golay, M. J. E. (1964).** Smoothing and differentiation of data by simplified least squares. *Analytical Chemistry*, 36(8), 1627–1639. Retrieved from <https://doi.org/10.1021/ac60214a047>

**Sousa, J. B., Craus, J., & Monismith, C. L. (1991).** Summary report on permanent deformation in asphalt concrete. *Journal of Transportation Engineering*, 117(1), 35–53. Retrieved from [https://doi.org/10.1061/\(ASCE\)0733-947X\(1991\)117:1\(35\)](https://doi.org/10.1061/(ASCE)0733-947X(1991)117:1(35))

**Thom, N. (2014).** *Principles of pavement engineering* (2nd ed.). Chichester, UK: Wiley. Retrieved from <https://doi.org/10.1002/9781118425145>

**Transport Research Laboratory. (2004).** *Overseas road note 40: Guide to axle load surveys*. Crowthorne, UK: Author.

**Ullidtz, P. (1998).** *Pavement analysis and design*. New York, NY: Wiley.

**Wang, H., & Al-Qadi, I. L. (2013).** Impact of tire loading on pavement response. *International Journal of Pavement Engineering*, 14(2), 119–131. Retrieved from <https://doi.org/10.1080/10298436.2011.653571>

**Wirtgen Group. (2010).** *Hawkeye 2000 series: User manual*. Windhagen, Germany: Author.

**Zhang, J., & Li, V. C. (2002).** Simulation of crack propagation in asphalt pavements. *Fatigue & Fracture of Engineering Materials & Structures*, 25(8), 947–957. Retrieved from <https://doi.org/10.1046/j.1460-2695.2002.00563.x>

## APPENDIXES

**Appendix A:** Visual and surface condition surveys, including a pavement condition summary detailing distress types and PCI ratings (Table A1). Additional details are available in the supplementary material at: [https://drive.google.com/file/d/19ceADfgeUs62xivikaUGm7S\\_dwSKOOwu/view?usp=sharing](https://drive.google.com/file/d/19ceADfgeUs62xivikaUGm7S_dwSKOOwu/view?usp=sharing).

**Appendix F:** Pavement Condition Metrics showing Road Slope, Mean Rut, Mean IRI and PCI Values in (Table F1), the slope categories along the case study sections, total distance by slope category in (Table F2), Terrain analysis visualizations, including a bar chart (Figure F1) and pie chart (Figure F2) of terrain distribution by slope category (flat, rolling, steep). Table F3: Shear Stress, Strength, and Safety Margins for LHS and RHS, Table F4: Rutting Depths (mm) and Compliance Uphill Acceleration (1 m/s<sup>2</sup>): LHS, Table F5: Rutting Depths (mm) and Compliance Uphill Acceleration (1 m/s<sup>2</sup>): RHS, Table F6: Rutting Depths (mm) and Compliance Uphill Deceleration (2 m/s<sup>2</sup>): LHS, and Table F7: Rutting Depths (mm) and Compliance Uphill Deceleration (2 m/s<sup>2</sup>): RHS. Additional details are available in the supplementary material at: [https://drive.google.com/file/d/19ceADfgeUs62xivikaUGm7S\\_dwSKOOwu/view?usp=sharing](https://drive.google.com/file/d/19ceADfgeUs62xivikaUGm7S_dwSKOOwu/view?usp=sharing).

For Figures: F1, F2 Tables: A1, F1, F2, F3, F4, F5, F6 and F7 Additional details are available in the supplementary material at: [https://drive.google.com/file/d/19ceADfgeUs62xivikaUGm7S\\_dwSKOOwu/view?usp=sharing](https://drive.google.com/file/d/19ceADfgeUs62xivikaUGm7S_dwSKOOwu/view?usp=sharing).



## APPENDIX A

Table A1: Pavement condition summary, including distress types and PCI ratings

Road Section	Chainage (km)	Sub Chainage (km)	IRI Right	IRI Left	IRI Avg	IRI Lane	IRI Rating	Rut Right	Rut Left	Avg Rut	Rut Lane	Rut Rating	PCI value	PCI rating	Bump Int	Speed (km/h)	Survey Time
A8 (I) LHS	0.1	0.1	4.88	3.5	4.19	3.64	0	1.562	3.26	2.413	3.992	0	56.93244	Fair	3348	35.2	12:43:48
A8 (I) LHS	0.2	0.2	3.97	3.74	3.85	3.62	0	2.508	2.86	2.684	4.249	0	57.06937	Fair	3220	38.1	12:43:48
A8 (I) LHS	0.3	0.3	3.69	3.65	3.67	3.22	0	2.039	4.98	3.507	5.801	0	60.05855	Fair	2832	46.3	12:43:48
A8 (I) LHS	0.4	0.4	3.53	4.05	3.79	3.46	0	1.23	4.85	3.038	5.368	0	58.20534	Fair	2785	53.2	12:43:48
A8 (I) LHS	0.5	0.5	1.44	1.53	1.48	1.23	0	6.942	1.66	4.303	7.218	1	91.36953	Good	1070	55.3	12:43:48
A8 (I) LHS	0.6	0.6	1.36	1.36	1.36	1.14	0	1.155	2.68	1.918	3.412	0	94.44729	Good	1037	55	12:43:48
A8 (I) LHS	0.7	0.7	1.87	1.9	1.89	1.7	0	0.437	2.44	1.438	2.589	0	79.34586	Satisfactory	1364	49.7	12:43:48
A8 (I) LHS	0.8	0.8	2.77	3.55	3.16	3.01	0	1.636	3.21	2.422	4.186	0	61.85076	Fair	2359	40.3	12:43:48
A8 (I) LHS	0.9	0.9	1.98	1.98	1.98	1.73	0	1.422	5.17	3.298	5.615	0	78.74299	Satisfactory	1320	36.2	12:43:48
A8 (I) LHS	1	1	1.68	1.41	1.55	1.36	0	0.74	2.74	1.741	3.038	0	87.45347	Good	1045	41.2	12:43:48
A8 (I) LHS	1.1	1.1	1.6	1.6	1.6	1.32	0	7.129	2.67	4.901	7.7	1	88.59919	Good	954	58.7	12:43:48
A8 (I) LHS	1.2	1.2	1.62	2	1.81	1.65	0	0.319	4.42	2.367	4.454	0	80.38537	Satisfactory	1331	60.7	12:43:48
A8 (I) LHS	1.3	1.3	1.59	1.52	1.55	1.3	0	0.502	3.25	1.874	3.378	0	89.19093	Good	1003	58.4	12:43:48
A8 (I) LHS	1.4	1.4	1.97	2.05	2.01	1.75	0	0.274	3.97	2.123	4.046	0	78.34935	Satisfactory	1368	58.5	12:43:48
A8 (I) LHS	1.5	1.5	1.95	1.82	1.88	1.67	0	2.373	2.42	2.395	4.365	0	79.9642	Satisfactory	1372	56.7	12:43:48
A8 (I) LHS	1.6	1.6	2.04	1.91	1.98	1.76	0	1.964	0.03	0.998	1.977	0	78.15495	Satisfactory	1486	54.3	12:43:48
A8 (I) LHS	1.7	1.7	1.96	1.76	1.86	1.63	0	0.943	1.53	1.236	2.109	0	80.81393	Satisfactory	1261	55.5	12:43:48
A8 (I) LHS	1.8	1.8	1.72	1.53	1.63	1.44	0	2.029	1.38	1.704	2.84	0	85.30097	Good	1108	43.1	12:43:48
A8 (I) LHS	1.9	1.9	2.26	2.53	2.4	2.24	0	0.971	1.17	1.07	1.792	0	70.3545	Satisfactory	1626	48.8	12:43:48
A8 (I) LHS	2	2	1.5	1.66	1.58	1.44	0	0.311	2.11	1.21	2.214	0	85.30097	Good	1242	63.8	12:43:48
A8 (I) LHS	2.1	2.1	1.69	1.65	1.67	1.45	0	0.304	1.65	0.977	1.765	0	85.04397	Good	1220	73.3	12:43:48
A8 (I) LHS	2.2	2.2	1.9	2.02	1.96	1.55	0	1.664	0.78	1.222	2.077	0	82.60672	Satisfactory	1204	69.6	12:43:48
A8 (I) LHS	2.3	2.3	2.42	2.55	2.48	2.29	0	1.671	1.22	1.448	2.618	0	69.68058	Fair	1594	63.4	12:43:48
A8 (I) LHS	2.4	2.4	1.97	1.78	1.87	1.62	0	1.487	1.64	1.565	2.696	0	81.03105	Satisfactory	1372	63.8	12:43:48
A8 (I) LHS	2.5	2.5	1.22	1.32	1.27	1.03	0	0.44	2.36	1.399	2.383	0	98.71951	Good	863	72	12:43:48
A8 (I) LHS	2.6	2.6	2.06	2.33	2.19	1.94	0	1.667	0.3	0.982	1.793	0	74.90632	Satisfactory	1415	77	12:43:48
A8 (I) LHS	2.7	2.7	2.55	2.53	2.54	2.35	0	1.715	0.3	1.007	1.925	0	88.89924	Fair	1761	71.7	12:43:48
A8 (I) LHS	2.8	2.8	2.71	2.36	2.53	2.26	0	0.522	0.25	0.388	0.745	0	70.08236	Satisfactory	1750	66.3	12:43:48
A8 (I) LHS	2.9	2.9	2.84	4.67	3.76	2.89	0	0.916	1.46	1.186	1.832	0	62.95765	Fair	2623	62.7	12:43:48
A8 (I) LHS	3	3	2.52	2.71	2.62	2.22	0	0.147	3.34	1.741	3.342	0	70.63015	Satisfactory	1807	58.5	12:43:48
A8 (I) LHS	3.1	3.1	2.74	2.88	2.81	2.5	0	2.159	0.56	1.359	2.311	0	67.06534	Fair	1932	56.5	12:43:48
A8 (I) LHS	3.2	3.2	2.43	2.78	2.6	2.45	0	0.265	2.02	1.141	2.111	0	67.65889	Fair	1875	55.1	12:43:48
A8 (I) LHS	3.3	3.3	2.46	2.47	2.47	2.34	0	1.9	0.87	1.383	2.553	0	69.02746	Fair	1890	55.6	12:43:48
A8 (I) LHS	3.4	3.4	2.83	2.98	2.9	2.65	0	0.313	2.36	1.339	2.399	0	65.38299	Fair	2224	55.2	12:43:48
A8 (I) LHS	3.5	3.5	2.06	2.22	2.14	1.97	0	0.003	4.08	2.039	4.075	0	74.40682	Satisfactory	1587	65.8	12:43:48
A8 (I) LHS	3.6	3.6	1.91	2.17	2.04	1.8	0	0.146	3.36	2.053	3.966	0	77.39291	Satisfactory	1441	66.7	12:43:48
A8 (I) LHS	3.7	3.7	2.43	2.66	2.55	2.37	0	1.035	4.34	2.689	4.72	0	68.64513	Fair	2046	69.7	12:43:48
A8 (I) LHS	3.8	3.8	2.29	2.69	2.49	2.34	0	3.709	0.77	2.239	3.837	0	69.02746	Fair	1836	66.6	12:43:48
A8 (I) LHS	3.9	3.9	2.33	2.24	2.29	2.16	0	0.068	3.33	1.701	3.36	0	71.47895	Satisfactory	1720	60.7	12:43:48
A8 (I) LHS	4	4	2.17	2.09	2.13	1.95	0	2.732	1.88	2.304	3.638	0	74.73859	Satisfactory	1449	56.2	12:43:48
A8 (I) LHS	4.1	4.1	2.89	3.01	2.95	2.8	0	0.595	4.2	2.399	4.388	0	63.83209	Fair	2103	53.8	12:43:48
A8 (I) LHS	4.2	4.2	1.96	2.45	2.21	1.96	0	2.051	1.91	1.98	3.392	0	74.5721	Satisfactory	1390	53.8	12:43:48
A8 (I) LHS	4.3	4.3	1.63	2.23	1.93	1.69	0	1.495	1.69	1.595	2.714	0	79.55022	Satisfactory	1252	47	12:43:48
A8 (I) LHS	4.4	4.4	2.21	1.92	2.06	1.75	0	3.139	2.25	2.694	4.75	0	78.34935	Satisfactory	1320	43.2	12:43:48
A8 (I) LHS	4.5	4.5	2.38	2.35	2.36	2.11	0	5.812	1.99	3.903	7.263	1	72.21258	Satisfactory	1424	35.6	12:43:48
A8 (I) LHS	4.7	4.7	1.87	2.04	1.96	1.65	0	0.3	0.77	0.536	0.948	0	80.38537	Satisfactory	1419	48.9	12:43:48
A8 (I) LHS	4.8	4.8	2.35	2.46	2.41	2.16	0	0.13	1.19	0.661	1.248	0	71.47895	Satisfactory	1826	50.5	12:43:48
A8 (I) LHS	4.9	4.9	3.41	3.42	3.42	3.12	0	0.123	2.52	1.321	2.533	0	60.89037	Fair	2102	45.6	12:43:48
A8 (I) LHS	5.1	5.1	2.72	3.03	2.87	2.78	0	0.523	4.07	2.298	4.179	0	64.03191	Fair	2005	22.9	12:43:48
A8 (I) LHS	5.2	5.2	3.19	3.27	3.23	3.08	0	0.23	2.69	1.459	2.697	0	61.2339	Fair	2417	44	12:43:48
A8 (I) LHS	5.3	5.3	2.48	2.24	2.36	2.21	0	0.922	3.22	2.072	3.468	0	70.76931	Satisfactory	1702	54.3	12:43:48
A8 (I) LHS	5.4	5.4	1.66	1.88	1.77	1.56	0	0.173	4.82	2.496	4.823	0	82.37543	Satisfactory	1082	56.6	12:43:48
A8 (I) LHS	5.5	5.5	1.71	1.64	1.67	1.41	0	0.961	2.23	1.595	2.799	0	86.08757	Good	1080	52.8	12:43:48
A8 (I) LHS	5.6	5.6	1.99	1.97	1.98	1.78	0	1.098	5.48	3.289	5.752	0	77.77066	Satisfactory	1344	54.4	12:43:48
A8 (I) LHS	5.7	5.7	1.83	2.05	1.94	1.79	0	0.496	6.06	3.279	6.322	1	77.58113	Satisfactory	1291	60.8	12:43:48
A8 (I) LHS	5.8	5.8	1.57	1.5	1.53	1.42	0	1.029	3.35	2.187	3.471	0	85.82272	Good	1065	65.8	12:43:48
A8 (I) LHS	5.9	5.9	1.49	1.75	1.62	1.5	0	0.925	2.62	1.772	2.936	0	83.79618	Satisfactory	1043	69.3	12:43:48
A8 (I) LHS	6	6	1.55	1.81	1.68	1.53	0	0.594	1.38	0.988	1.674	0	83.0758	Satisfactory	1169	68.1	12:43:48
A8 (I) LHS	6.1	6.1	1.56	1.66	1.61	1.46	0	0.484	2.39	1.437	2.529	0	84.78952	Satisfactory	1057	65.3	12:43:48
A8 (I) LHS	6.2	6.2	1.62	1.77	1.7	1.52	0	1.649	2.48	2.062	3.4	0	83.31366	Satisfactory	1194	64.1	12:43:48
A8 (I) LHS	6.3	6.3	1.66	1.78	1.72	1.58	0	0.023	9.84	4.93	9.837	1	81.91916	Satisfactory	1100	63.6	12:43:48
A8 (I) LHS	6.4	6.4	1.77	1.88	1.83	1.57	0	0.79	5.63	3.219	5.763	0	82.14625	Satisfactory	1156	63.6	12:43:48
A8 (I) LHS	6.5	6.5	1.54	1.72	1.63	1.45	0	1.812	1.67	1.742	3.071	0	85.04397	Good	1040	64.8	12:43:48
A8 (I) LHS	6.6	6.6	2.01	2.1	2.05	1.88	0	0.843	2.76	1.801	3.028	0	75.9394	Satisfactory	1407	63.8	12:43:48
A8 (I) LHS	6.7	6.7	1.72	1.9	1.81	1.72	0	0.006	10.3	5.137	10.267	2	78.94227	Satisfactory	1151	63.7	12:43:48
A8 (I) LHS	6.8	6.8	1.67	1.81	1.74	1.57	0	1.125	4.09	2.61	4.114	0	82.14625	Satisfactory	1100	65.9	12:43:48
A8 (I) LHS	6.9	6.9	1.47	1.46	1.46	1.3	0	0.177	8.22	4.197	8.216	1	89.19093	Good	858	66.3	12:43:48
A8 (I) LHS	7	7	1.65	1.98	1.82	1.65	0	0.12	7.7	3.912	7.704	1	80.38537	Satisfactory	1084	65.8	12:43:48
A8 (I) LHS	7.1	7.1	1.58	1.81	1.69	1.55	0	0.023	7.71	3.868	7.712	1	82.60672	Satisfactory	998	63.1	12:43:48
A8 (I) LHS	7.2	7.2	1.99	1.97	1.98	1.77	0	0.157	6.17	3.161	6.188	1	77.96212	Satisfactory	1307	60.5	12:43:48
A8 (I) LHS	7.3	7.3	1.82	2.11	1.96	1.81	0	0.033	4.92	2.477	4.92	0	77.20619	Satisfactory	1288	52.2	12:43:48
A8 (I) LHS	7.4	7.4	2.62	2.93													

## APPENDIX B: Traffic volume survey report

Table B1: Traffic count data for Mau Summit-Timboroa A8

TIMBOROA - NAIKROI JUNCTION TRAFFIC COUNT DATA														
Lane	Vehicle Type	Day-1	Day-2	Day-3	Day-4	Day-5	Day-6	Day-7	ADT					
		26-Aug-24	27-Aug-24	28-Aug-24	29-Aug-24	30-Aug-24	31-Aug-24	1-Sep-24						
		Mon	Tue	Wed	Thu	Fri	Sat	Sun						
LHS	Hand-cart	-	-	-	-	-	-	-	-					
	Animal-Cart	-	-	-	-	-	-	-	-					
	Bicycles	-	-	-	-	-	-	-	-					
	Motor bikes	150	150	173	76	176	127	172	146					
	Tuk tuk	-	-	-	-	-	-	-	-					
	Cars	1,148	1,055	692	817	868	888	1,060	933					
	Micro bus	50	335	335	264	89	421	465	280					
	Mini Buses	1,383	1,568	1,107	771	1,783	1,131	966	1,236					
	Bus	138	99	148	135	240	182	214	162					
	Omni bus	103	58	60	156	206	125	62	110					
	Pick up	56	207	193	176	188	419	387	232					
	LGV	143	216	51	141	316	154	169	170					
	MGV	336	489	492	834	1,073	672	684	654					
	HGV1	58	122	91	266	329	292	111	184					
	HGV2	1,144	1,001	1,038	863	1,210	1,243	1,110	1,087					
	Tractors	11	10	3	8	3	-	-	3					
	TOTAL	4,721	6,290	4,388	4,829	6,479	6,827	8,167						

15 - 24 HR RATIO	Bicycles	Motor bikes	Tuk tuk	Cars	Micro bus	Mini Buses	Bus	Omni bus	Pick up	LGV	MGV	HGV1	HGV2	Tractors
WEEKDAY	1.30	1.30		1.40	1.20	1.10	1.40	1.20	1.10	1.30	1.30	1.30	1.60	1.30
WEEKEND	1.10	1.10		1.20	1.10	1.10	1.10	1.20	1.10	1.20	1.40	1.20	1.30	1.00

DAY	Bicycles	Motor bikes	Tuk tuk	Cars	Micro bus	Mini Buses	Bus	Omni bus	Pick up	LGV	MGV	HGV1	HGV2	Tractors	TOTAL
MON	0	195	0	1492	465	1798	179	134	73	186	437	75	1485	14	6337
TUE	0	195	0	1371	436	2038	103	75	270	281	635	159	1301	13	6877
WED	0	225	0	900	436	1439	192	78	251	66	640	118	1349	7	5701
THU	0	99	0	1062	343	1003	176	203	229	183	1083	372	1122	10	5887
FRI	0	228	0	1129	115	2237	312	268	244	410	1393	438	1573	4	6623
SAT	0	140	0	977	463	1244	200	138	461	169	739	321	136	0	6238
SUN	0	189	0	1166	512	997	235	68	425	186	753	122	1221	0	5874
TOTAL	0	1291	0	8696	2269	10837	1397	964	1083	1482	4684	1896	9421	48	45118
ADT	0	182	0	1119	338	1548	208	138	279	212	812	228	1346	7	6445
%	0	3	0	18	8	24	3	2	4	3	13	4	21	0	100
PCU Factor	0.5	1.0	1.0	1.0	1.5	1.5	1.5	4.0	1.0	1.5	5.0	8.0	8.0	3.0	
Year 10 PCU	0	182	0	1119	338	1548	208	138	279	212	812	228	1346	7	6445

RHS	Hand-cart	-	-	-	-	-	-	-	-					
	Animal-Cart	-	-	-	-	-	-	-	-					
	Bicycles	-	-	-	-	-	-	-	-					
	Motor bikes	369	263	79	198	115	41	204	181					
	Tuk tuk	-	-	-	-	-	-	-	-					
	Cars	1,502	1,122	560	632	814	754	1,074	923					
	Micro bus	65	91	87	76	381	67	495	180					
	Mini Buses	1,584	954	735	564	799	1,033	1,294	961					
	Bus	217	182	172	123	91	70	132	141					
	Omni bus	26	23	112	41	18	77	92	35					
	Pick up	135	144	306	107	258	350	220	217					
	LGV	72	77	125	37	177	397	206	115					
	MGV	275	369	544	384	464	613	690	508					
	HGV1	397	142	61	168	491	135	108	214					
	HGV2	1,285	1,233	946	1,134	1,243	1,113	1,683	1,275					
	Tractors	32	18	18	24	4	14	8	17					
	TOTAL	6,988	6,131	3,788	3,697	4,818	4,368	6,007						

15 - 24 HR RATIO	Bicycles	Motor bikes	Tuk tuk	Cars	Micro bus	Mini Buses	Bus	Omni bus	Pick up	LGV	MGV	HGV1	HGV2	Tractors
WEEKDAY	1.30	1.30		1.40	1.20	1.10	1.40	1.20	1.10	1.30	1.30	1.30	1.60	1.30
WEEKEND	1.10	1.10		1.20	1.10	1.10	1.10	1.20	1.10	1.20	1.40	1.20	1.30	1.00

DAY	Bicycles	Motor bikes	Tuk tuk	Cars	Micro bus	Mini Buses	Bus	Omni bus	Pick up	LGV	MGV	HGV1	HGV2	Tractors	TOTAL
MON	0	479	0	1933	84	2059	283	33	175	94	357	515	1671	42	7745
TUE	0	342	0	1438	119	1245	256	30	187	100	766	183	1980	23	6671
WED	0	103	0	788	113	956	234	146	398	163	707	79	1234	23	4882
THU	0	237	0	822	99	934	160	53	139	74	499	211	1474	31	4662
FRI	5	130	0	1059	496	987	118	24	335	222	603	638	1616	3	6259
SAT	4	45	0	829	74	1136	77	85	385	107	674	149	1224	15	4805
SUN	0	224	0	1182	545	1205	145	101	242	227	759	119	1851	9	6607
TOTAL	25	1660	0	8031	1829	8325	1243	471	1861	966	4366	1903	11646	149	43329
ADT	3	229	0	1127	218	1189	178	67	266	141	624	272	1878	21	5983
%	0	4	0	19	4	20	3	1	4	2	11	8	24	0	100
PCU Factor	0.5	1.0	1.0	1.0	1.5	1.5	1.5	4.0	1.0	1.5	5.0	8.0	8.0	3.0	

Source: Field survey, 2025

## APPENDIX C: Coring test results

Table C1: Asphalt concrete core samples

ASPHALT CONCRETE CORE ANALYSIS																		
Sample No.	ROAD NAME	Sampling Location	Core Thickness	Core Density	Max. Theoretical Density	Core air voids	Binder Content	Particle size distribution (% passing)										
		CH	mm	(g/cc)	(g/cc)	(%)	(%)	28	20	14	10	6.3	4	2	1	0.425	0.3	0.15
1	Mau s - timboroa	13+500 LHS	54	2.346	2.517	6.8	5.0	100	100	94	70	55	43	32	22	14	11	9
2		33+500 RHS	50	2.424	2.500	3.0	5.1	100	100	90	76	59	45	32	20	12	11	9

Source: Field survey, 2025



Table C2: DBM Core samples

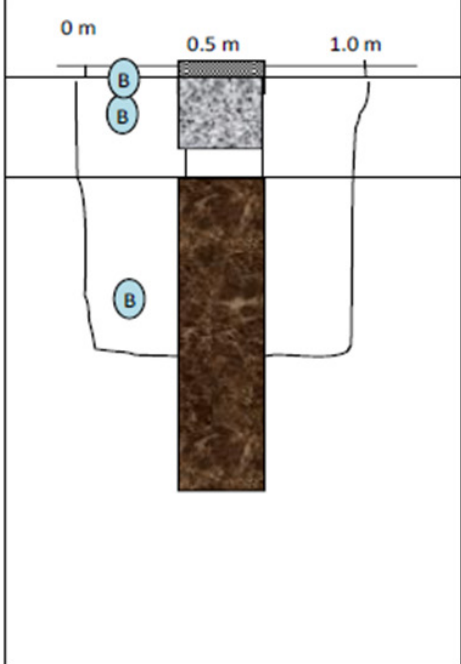

		DBM CORE ANALYSIS														
Sample No.	Road name	Sampling Location	Core Thickness	Core Density	Max. Theoretical Density	Core air voids	Binder Content	Particle size distribution (% passing)								
								37.5	28	20	14	6.3	2	1	300	0.075
		CH	mm	(g/cc)	(g/cc)	(%)	(%)									
1	Mau s-Timboroa	13+500 LHS	155	2.329	2.504	7.0	4.0	100	95	84	63	47	28	19	10	6
2		33+500 RHS	180	2.366	2.525	6.3	4.1	100	100	88	79	59	39	26	12	6

Source: Field survey, 2025

**APPENDIX D**

Table D1: Trenching Results

Chainage: KM 13+500 LHS TP1 Coordinates: S 003'57.34.331" &amp; E 35038'34.26358"

		Depth, cm	Description of face and material
			Surface dressing <b>10mm</b>
			Surfacing: Asphalt wearing course, <b>55 mm</b> thick
			Base: Dense bitumen macadam <b>160 mm</b> thick.
			Sub base: Graded crushed stones <b>270 mm</b> thick.
			Top subgrade: Brownish gravel, <b>150mm</b> thick.
			Bottom subgrade: Brownish gravel, <b>150+ mm</b> thick.
			<b>Pavement layer thickness=495 mm</b>
Notes	Sampling	Plan or photo of the pit	
Layer 1: Bituminous Material ○ sampled & tested Layer 2: Graded crushed stones, sub base. ○ Not Sampled Layer 3: Brownish gravel, Top Subgrade. ○ Sampled & Tested Layer 4: Brownish gravel, Bottom Subgrade. ○ Sampled & Tested.  <b>NB:</b> This area has developed longitudinal cracks	(J)  Jar Sample (B)  Bulk Sample (N)  Not Sampled		

Source: Field survey, 2025



## APPENDIX E

Table E1: Traffic speed survey summary

Survey Location	Makataan Junction	Timboroa Bridge	Mlango 4	Ekwen	Hilltea
Average Road Grade (%)	5.8%	9.7%	5.7%	4.5%	4.8%
Mean ( $\bar{X}$ )	23	21	19	20	20
$\Sigma (x - \bar{x})^2$	5841	2588	2049	1213	2996
n	181	240	240	185	261
$\Sigma (x - \bar{x})^2/n$	32	11	9	7	11
Std Deviation	6	3	3	3	3
85th Percentile	28.0	25.0	22.0	22.4	24.0
No of Speeders	21	23	28	28	0
Proportion of Speeders	0.1	0.1	0.1	0.2	0.0
Average of Speeders	23	21	19	20	20

Source: Field survey, 2025

## APPENDIX F

Table F1: Slope and distress correlation for Mau Summit-Timboroa A8

Road Section	Locations	Chainage (km)	Road slope (%)	Mean Rut	Mean IRI	PCI value
A8 (1) LHS	Mau Summit Interchange	0.1	2.30%	2.413	4.19	56.93244
A8 (1) LHS		0.2	2.30%	2.684	3.85	57.06937
A8 (1) LHS		0.3	2.30%	3.507	3.67	60.05855
A8 (1) LHS		0.4	-2.20%	3.038	3.79	58.20534
A8 (1) LHS		0.5	-2.20%	4.303	1.48	91.36953
A8 (1) LHS		0.6	2.80%	1.918	1.36	94.44729
A8 (1) LHS		0.7	2.80%	1.438	1.89	79.34586
A8 (1) LHS		0.8	2.80%	2.422	3.16	61.85076
A8 (1) LHS		0.9	2.80%	3.298	1.98	78.74299
A8 (1) LHS		1	2.80%	1.7405	1.55	87.45347
A8 (1) LHS		1.1	3.70%	4.9005	1.6	88.59919

A8 (1) LHS		1.1	3.70%	4.9005	1.6	88.59919
A8 (1) LHS		1.2	3.70%	2.367	1.81	80.38537
A8 (1) LHS		1.3	3.70%	1.8735	1.55	89.19093
A8 (1) LHS		1.4	3.70%	2.123	2.01	78.34935
A8 (1) LHS		1.5	3.70%	2.395	1.88	79.9642
A8 (1) LHS		1.6	1.50%	0.998	1.98	78.15495
A8 (1) LHS		1.7	1.50%	1.2355	1.86	80.81393
A8 (1) LHS		1.8	1.50%	1.704	1.63	85.30097

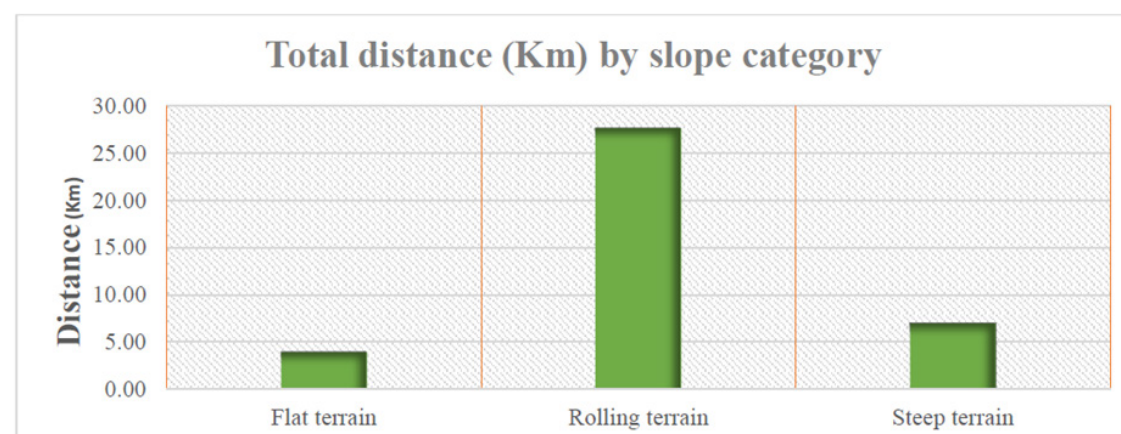
Source: Field survey, 2025

Table F2: Slope category

Slope category			Distance (km)	
<b>Steep sections</b>	gradient > 5%	18%	6.99	6
<b>Rolling terrain</b>	gradient 2-5%	72%	27.66	1
<b>Nearly flat terrain</b>	gradient < 2%	10%	3.95	10
		100%	38.61	

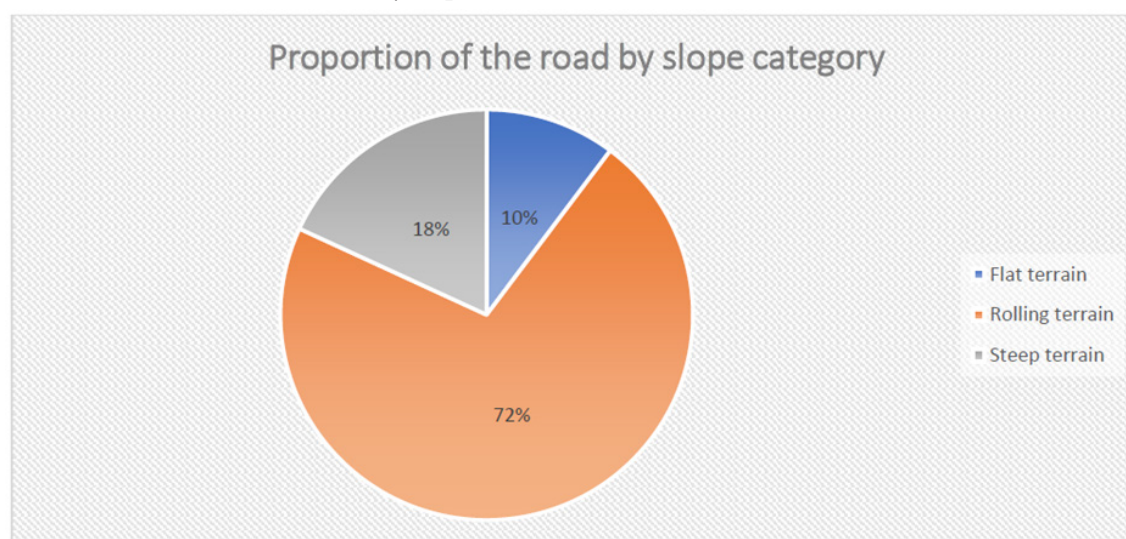
Source: Field survey, 2025

Table F1: Bar Chart of distance by slope



Source: Field survey, 2025

Table F2: Pie Chart of the Road by slope



Source: Field survey, 2025

## APPENDIX G

### Python Code Snippet

Python Code Snippet:

```
import pandas as pd
import matplotlib.pyplot as plt
from scipy.signal import savgol_filter

#-----#-----#-----#-----#-----#
#-----#-----#-----#-----#-----#

# Load the dataset from an Excel file
# Ensure the file 'Moses.xlsx' is in the same directory as this script
dataframe1 = pd.read_excel('Moses.xlsx')

# Rename columns for better readability
# 'Chainage (km)' represents distance along the road, renamed as 'X'
# 'road slope (%)' represents the slope percentage, renamed as 'Y'
dataframe1.rename(columns='Chainage (km)': 'X', 'road slope (%)': 'Y', inplace=True)
```

```

# Display the first few rows of the dataset to verify the data
print("First few rows of the dataset:")

# Print the first 20 (x,y) points
print(dataframe1.head(20))

#-----#-----#-----#-----#-----#
#-----#-----#-----#-----#-----#

# Plot the raw data points
plt.figure(figsize=(30, 10))

plt.scatter(dataframe1['X'], dataframe1['Y'], color='blue', label='Data Points', alpha=0.6)
plt.plot(dataframe1['X'], dataframe1['Y'], linestyle='-', color='gray', alpha=0.7) # Line
connecting raw points

# Add plot labels and grid for better readability
plt.title("Road Slope vs. Chainage (Raw Data)")
plt.xlabel("Road Slope (%)")
plt.ylabel("Chainage (km)")
plt.grid(True)
plt.legend()
plt.savefig('Plot1')
plt.show()

#-----#-----#-----#-----#-----#
#-----#-----#-----#-----#-----#

# Apply Savitzky-Golay filter to smooth the 'Y' values
# The filter helps to reduce noise and better visualize trends
window_size = 11 # Window size must be an odd number
poly_order = 2 # Polynomial order for the filter
dataframe1['Y_smooth'] = savgol_filter(dataframe1['Y'], window_size, poly_order)
# Plot the original data points along with the smoothed curve
plt.figure(figsize=(30, 10))

plt.scatter(dataframe1['X'], dataframe1['Y'], color='blue', label='Original Data', alpha=0.6)
plt.plot(dataframe1['X'], dataframe1['Y_smooth'], color='red', linestyle='-', linewidth=2,
label='Smoothed Curve')

```



```
# Customize the plot with labels, grid, and legend  
plt.title("Road Slope vs. Chainage (Smoothed Data)")  
plt.xlabel("Road Slope (%)")  
plt.ylabel("Chainage (km)")  
plt.grid(True)  
plt.legend()  
plt.savefig('Plot2')  
  
# Display the final plot  
plt.show()
```